Few-Body Systems 3, 123–134 (1988)

Few-Body Systems

Elastic Scattering and Break-Up Processes in the *n-d* System

H. Witała*, T. Cornelius, and W. Glöckle

Institut für Theoretische Physik, Ruhr-Universität Bochum, Universitätsstrasse 150, D-4630 Bochum, Federal Republic of Germany

Abstract. A method to solve the AGS equations in momentum space is presented. The two-nucleon transition operators are generated with the new Bonn potential restricted to the states $^1S_0$, $^3S_1$-$^3D_1$, $^3P_0$, $^1P_1$, $^3P_1$, $^3P_2$-$^3F_2$, $^1D_2$ and $^3D_2$. Cross sections and analyzing powers for elastic and break-up processes are calculated at a neutron laboratory energy $E_n = 10.3$ MeV.

1 Introduction

The traditional approach to nuclear physics is based on a nonrelativistic Hamiltonian in which the nucleons interact pairwise. There are different two-nucleon interactions, purely phenomenological ones (as, for instance, the Reid soft-core potential [1]) and ones based on meson exchanges (as, for instance, the Paris [2] and Bonn [3] potentials), which, when applied in such a model, describe the two-nucleon system with about the same, rather good, accuracy.

Using that model in the bound systems of 3 and 4 nucleons those interactions underbind ^{3}H by about 1 to 1.5 MeV [4, 5] and ^{4}He by about 4 to 7 MeV [6]. The OBE-parametrization of the new Bonn potential [7] breaks that situation the first time and yields a higher binding energy for ^{3}H [8]. On the other hand three-nucleon forces could be responsible for the discrepancy between experimental and theoretical binding energies. This is indicated by recent calculations based on the 2π-exchange three-nucleon force [9] and phenomenological ansätze [10]. In order to get additional information more three-nucleon observables are needed. There are ones which scale with the ^{3}H binding energy like the radius of ^{3}H, the ratio of asymptotic D/S normalization constants in the ^{3}H wave function, the doublet *n-d* scattering length and others [5] and therefore yield no additional information. However, this can be different in the three-nucleon system at positive energies. There the emphasis on different force components can be varied from the ones which play the dominant role in the ^{3}H ground state. For instance, polarization data in elastic *n-d* scattering depend sensitively on *p*-wave forces. Also in the break-up process very

* Alexander-von-Humboldt Fellow. *Permanent address:* Institute of Physics, Jagellonian University, PL-130059 Cracow, Poland

different geometrical configurations for 3 outgoing nucleons can be chosen which clearly test the tails of a three-body wave function differently and in much more detail than for instance a root-mean-square radius for a bound state.

Further support for more careful studies of the three-nucleon system comes also from a recent work [11] which compares the sensitivity of two-nucleon force off-shell effects in ^{3}H to those effects in ^{4}He and nuclear matter. The conclusion is that the three-nucleon system is most sensitive.

The theoretical framework for three-body systems was originally laid by Faddeev [12]. Important qualitative insight into three-body scattering processes was gained along the line initiated by Amado [13] and Lovelace [14], who simplified the formalism by using separable approximations to two-body transition operators. Today most calculations are based on the AGS form [15] of three-body equations. Due to computer limitations the first three-nucleon scattering calculations have been made with separable approximations to two-body interactions. This approach has reached now a high degree of sophistication [16] and has proved to be quite successful in describing experimental data [17, 18]. However, there are discrepancies between calculations and experiment, especially for high-accuracy polarization data (A_y^n) at low neutron energies [18]. Among possible explanations for those discrepancies there is still the purely technical uncertainty about the quality of describing a given realistic potential by finite-rank approximations. So before attributing the discrepancies for A_y^n to wrong off-shell (and on-shell) behaviour of two-nucleon or even the action of three-nucleon forces the theoretical results have to be established rigorously without using separable approximations to the given force. Pioneering work in this direction has been undertaken by Kloet and Tjon [19], Stolk and Tjon [20], Benayoun et al. [21]. More recently that difficult problem has been attacked by Takemiya [22] and Brandenburg [23].

Progress in experimental techniques makes it possible to perform kinematically complete measurements of break-up processes induced by polarized neutrons [24]. To plan such complicated experiments a theoretical guidance is needed to select those configurations which are sensitive for instance to off-shell effects. Therefore rigorous calculations using realistic meson-theoretical interactions are needed.

In this paper we present cross sections and analyzing powers for elastic scattering and break-up processes in the *n-d* system for a neutron lab energy of 10.3 MeV. They are obtained by solving the AGS equations in momentum space using the new Bonn potential. In Sect. 2 we describe briefly the formalism. The detailed techniques solving the system of equations are presented in Sect. 3. Our results and conclusions are given in Sect. 4.

2 Formalism

We would like to describe processes originating from bombarding deuterons by neutrons. We regard the three nucleons as identical and assume that they interact by pairwise interactions V. Then the problem can be reduced to the solution of the AGS equation for the elastic scattering transition operator U [25]:

$$U = PG_0^{-1} + PtG_0U\,. \tag{1}$$

Here G_0 is the free propagator

$$G_0 = \frac{1}{E + i0 - H_0} \tag{2}$$

and E the total center-of-mass energy fixed by the initial momentum of the neutron relative to the deuteron, $\mathbf{q}_0$, and the binding energy of the deuteron, E_d (we choose $\hbar = 1$)

$$E = \frac{3}{4m}\mathbf{q}_0^2 + E_d. \tag{3}$$

The operator t is a solution of the Lippmann-Schwinger equation

$$t = V + VG_0t \tag{4}$$

and P is the sum of two permutation operators

$$P = P_{12}P_{23} + P_{13}P_{23}. \tag{5}$$

The transition operator for the break-up process U_0 can be calculated once U is known,

$$U_0 = (1 + P)tG_0U. \tag{6}$$

The main problem with solving (1) in momentum space is the presence of singularities in t and G_0. Even more unpleasant is the action of P in (1) which smears out the pole in t, occurring at the deuteron binding energy, into a logarithmic singularity. The latter difficulty can be avoided by replacing (1) by [26]:

$$T = tP + tG_0PT. \tag{7}$$

Then the transition operator for elastic scattering U can be expressed as

$$U = PG_0^{-1} + PT. \tag{8}$$

We introduce standard Jacobi momenta and partial-wave basis states (see Fig. 1):

$$|pq\alpha\rangle \equiv |pq(ls)j(\lambda\tfrac{1}{2})IJ(t\tfrac{1}{2})T\rangle. \tag{9}$$

In that representation Eq. (7) is an infinite system of coupled integral equations [25]

$$\begin{aligned}\langle pq\alpha|T(E)|\phi\rangle = {} & \langle pq\alpha|tP|\phi\rangle \\ & + \sum_{\alpha'}\sum_{l_{\tilde{\alpha}}}\int_0^\infty dq'\,q'^2\int_{-1}^{1}dx\,\frac{\langle pl_\alpha|t^{(\alpha)}\left(E-\frac{3}{4m}q^2\right)|\pi_1 l_{\tilde{\alpha}}\rangle}{\pi_1^{l_{\tilde{\alpha}}}} \\ & \times\frac{G_{\tilde{\alpha}\alpha'}(q,q',x)}{\pi_2^{l_{\alpha'}}}\,\frac{\langle\pi_2 q'\alpha'|T(E)|\phi\rangle}{E+i0-q^2-q'^2-qq'x}.\end{aligned} \tag{10}$$

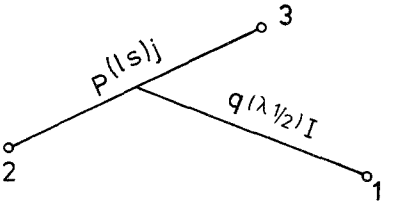

Fig. 1. Choice of Jacobi momenta and definition of the angular-momentum coupling scheme

The ket $|\phi\rangle = |\psi_{m_d}, \mathbf{q}_0, m_n\rangle$ describes the initial state of a neutron and a deuteron having spin projections m_n and m_d, respectively. The off-shell matrix elements

$$\langle pl_\alpha | t^{(\alpha)}\left(E - \frac{3}{4m}q^2\right)|\pi_1 l_{\bar{\alpha}}\rangle$$

of the two-body t-operator are obtained from (4). The geometrical coefficients $G_{\bar{\alpha}\alpha'}(q, q', x)$ and the momenta $\pi_1 = \sqrt{q'^2 + 0.25q^2 + qq'x}$, $\pi_2 = \sqrt{q^2 + 0.25q'^2 + qq'x}$ stem from the matrix elements $\langle pq\alpha|P|p'q'\alpha'\rangle$ of the permutation operator P [25]. The quantum numbers in the set $\bar{\alpha}$ differ from those in α only in the orbital angular momentum l of the pair. This change in l occurs only when the tensor force is acting.

The expression for the leading term $\langle pq\alpha|tP|\phi\rangle$ is given in the Appendix.

From the amplitudes $\langle pq\alpha|T|\phi\rangle$ the transition amplitudes for elastic $\langle \psi_{m'_d}, \mathbf{q}'_0, m'_n|U|\phi\rangle$ and the break-up process $\langle m_1 m_2 m_3 p_1 p_2 p_3|U_0|\phi\rangle$ with definite spin projections of the final particles are calculated by quadrature via (8) and (6), respectively. In a standard manner finally the unpolarized cross sections and polarization observables are obtained [20, 27].

3 Method of Solution

The first step is to truncate the infinite number of channels α in (10) to a finite one. For a given energy E the short-range two-body interaction V can be considered to be negligible beyond a certain total angular momentum $j_{\max}$ in the two-body subsystem. With increasing energy $j_{\max}$ will increase. Putting $t^{(\alpha)} = 0$ for $j > j_{\max}$ yields a finite number of channels for each total angular momentum J of the three-body system.

As mentioned in Sect. 2 the main problem of treating (10) is caused by the singularities of the two-body t-operator and the free propagator G_0. Only the two-body t-operator belonging to the ${}^3S_1$-${}^3D_1$ interaction, which supports a bound state, the deuteron, has a pole at the off-shell energy

$$E - \frac{3}{4m}q^2 = E_d.$$

In other words the pole occurs at $q = q_0$ and shows up in "deuteron"-like channels $\alpha_D = \{(l1)1(\lambda\tfrac{1}{2})IJ(0\tfrac{1}{2})\tfrac{1}{2}\}$ with $l = 0$ or 2. As is evident from (10) that pole appears also in $\langle pq\alpha_D|T|\phi\rangle$. This suggests the following definitions,

$$\langle pq\alpha|\hat{z}|\phi\rangle \equiv \begin{cases} \left(E - \frac{3}{4m}q^2 - E_d\right)\langle pq\alpha|z|\phi\rangle & \text{for} \quad \alpha = \alpha_D, \\ \langle pq\alpha|z|\phi\rangle & \text{for} \quad \alpha \neq \alpha_D, \end{cases} \tag{11}$$

where $z = T$, t or tP. Further putting

$$x_0 = \frac{mE - q^2 - q'^2}{qq'}, \tag{12}$$

we can rewrite (10) as

$$\langle pq\alpha|\hat{T}(E)|\phi\rangle = \langle pq\alpha|\hat{t}\left(E-\frac{3}{4m}q^2\right)P|\phi\rangle$$
$$+\sum_{\alpha'}\sum_{l_{\tilde{\alpha}}}\int_0^\infty dq'\,q'^2\int_{-1}^{1}dx\,\frac{\langle pl_\alpha|\hat{t}^{(\alpha)}\left(E-\frac{3}{4m}q^2\right)|\pi_1 l_{\tilde{\alpha}}\rangle}{\pi_1^{l_{\tilde{\alpha}}}}$$
$$\times\frac{G_{\tilde{\alpha}\alpha'}(q,q',x)}{\pi_2^{l_{\alpha'}}}\,\frac{m}{qq'(x_0+i0-x)}$$
$$\times\left[\langle\pi_2 q'\alpha'\neq\alpha_D|\hat{T}(E)|\phi\rangle+\frac{4}{3m}\,\frac{\langle\pi_2 q'\alpha'=\alpha_D|\hat{T}(E)|\phi\rangle}{q_0^2-q'^2}\right]. \quad (13)$$

This is the equation we solved. As in ref. [19, 23] the Neumann series is generated and summed up by the Padé method.

The shaded area shown in Fig. 2 comprises the q, q'-values for which $|x_0| \leqslant 1$. Thereby the maximal q (or q') value leading to a singularity is $q_{\max} = \sqrt{\frac{4}{3}mE}$. We treat that singularity by subtracting the integrand at $x = x_0$. Doing that throughout $0 < q, q' \leqslant q_{\max}$ leads to numerical inaccuracies since for small q-values x_0 can be very large and the Legendre polynomials $P_k(x_0)$ entering $G_{\tilde{\alpha}\alpha'}$ blow up with increasing J-values. Therefore the subtraction was performed only in the region $|x_0| \leqslant 1.2$ which is inside the solid line in Fig. 2. Then for $q \leqslant q_{\max}$ the integral over q' in (13) is broken up into 6 parts (see Fig. 2)

$$\int_0^\infty dq' = \int_0^{q_1} dq' + \int_{q_1}^{q_2} dq' + \int_{q_2}^{q_3} dq' + \int_{q_3}^{q_4} dq' + \int_{q_4}^{q_{\max}} dq' + \int_{q_{\max}}^{\infty} dq'. \quad (14)$$

The regularized integrand with respect to x can be integrated using 10 Gauß-Legendre quadrature points. The x-integral for the subtracted term can be performed analytically and leads to logarithmic singularities along the dashed line ($|x_0| = 1$) in Fig. 2. Again that singularity in q' was treated by the subtraction

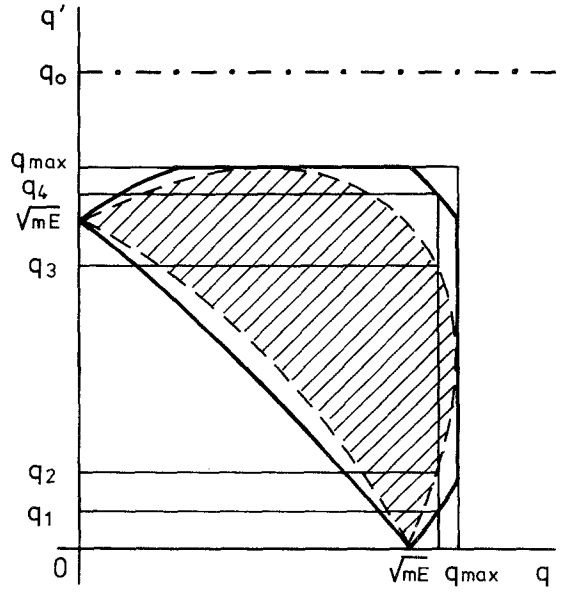

Fig. 2. The singularities in the q-q' plane together with the choice of integration intervals. Logarithmic singularities lie on the dashed lines. The pole at $q' = q_0$ arising from the deuteron bound state is shown by the dashed-dotted line. The regularizing in the x-integration was made in the region limited by the thick solid line

method. We perform the q'-integral for $0 \leqslant q' \leqslant q_{\max}$ using 26 quadrature points. Since the lengths of the subintervals and the behaviour of the integrands in these intervals are different for different q-values, the distribution of quadrature points has to be chosen appropriately. For the numerical results presented the minimal number of integration points for the subintervals $[0, q_1]$, $[q_1, q_2]$, $[q_2, q_3]$, $[q_3, q_4]$, $[q_4, q_{\max}]$ are 4, 3, 6, 3, 6, respectively. The remaining four points are distributed to different subintervals according to their lengths.

In the last interval $q_{\max} \leqslant q' < \infty$ we introduce a high enough cut-off at $q'_{\max} = 25\,\mathrm{fm}^{-1}$ and choose 16 quadrature points within $q_{\max} \leqslant q' \leqslant q'_{\max}$. The deuteron pole lying in this interval at $q' = q_0$ and occurring for channels $\alpha' = \alpha_D$ was again treated by the subtraction technique.

In the course of iterating the set (13) those integrals lead to terms in the Neumann series evaluated at certain p- and q-values. Thinking of the very many break-up configurations the matrix elements finally resulting have to be interpolated. For that purpose it is important to choose a good set of grid points, which includes certain special points. They are $q = 0$ and $q = q_{\max}$. The second case corresponds exactly to a configuration of a final-state interaction, where two nucleons have identical momenta. At the point $q = 0$ most of the problems presented above do not occur. Besides these two special points we choose 12 q-values in the interval $(0, q_{\max})$ with 3 points lying in the vicinity of $q_{\max}$. This is necessary to map out the very sharp slope in the amplitudes $\langle pq\alpha|\hat{T}|\phi\rangle$ and $\langle pl_\alpha|t^{(\alpha)}|\pi_1 l_{\tilde{\alpha}}\rangle$ for $q \to q_{\max}$ and channels including the two-body partial-wave state $^1S_0$. That slope is caused by the virtual-state pole of the $^1S_0$ two-body t-matrix. Based on this set of grid points we interpolate the amplitude $\langle \pi_2 q'\alpha|\hat{T}|\phi\rangle$ needed for the next iteration at the above-mentioned 26 quadrature points. This is done by spline interpolation [28]. Since the amplitude $\hat{T}$ behaves like $\hat{q} \equiv \sqrt{q_{\max}^2 - q'^2}$ for $q' \to q_{\max}$ we do not interpolate in q' but rather in $\hat{q}$.

Finally the discretization in the subsystem momentum p was done on a basis of 16 points distributed over the interval $(0, 25)\,\mathrm{fm}^{-1}$. Beyond $p = 25\,\mathrm{fm}^{-1}$ the two-body t-matrix is negligibly small. The interpolation of the amplitudes in (13) at the values π_1 and π_2 is again performed by splines.

Estimating numerical errors by changing the number of integration points and their distribution we find stability within 5%. As a further test we recalculated the cross sections for elastic scattering and break-up processes in the model of ref. [19] and find agreement within less than 3%.

4 Results and Conclusions

The presented method is applied to the n-d system at $E_n = 10.31$ MeV lab energy. Sensitivity studies at $E_n = 10.0$ MeV are also reported. This work is meant to demonstrate the techniques and feasibility. We present first results but defer the full application of our program to a forthcoming publication. In this study we assume the pair interaction V to act in the states $^1S_0$, $^3S_1$-$^3D_1$, $^3P_0$, $^1P_1$, $^3P_1$, $^3P_2$-$^3F_2$, $^1D_2$, $^3D_2$ (large set) and $^1S_0$, $^3S_1$-$^3D_1$, $^3P_0$, $^3P_1$ (small set), respectively. The potential chosen is the OBE parametrization of the new Bonn potential [7].

The theoretical differential cross section for elastic scattering is shown in Fig. 3 (solid line) together with experimental data from [29] taken at $E_n = 10.25$ MeV. Though the energies are a bit different there will remain a discrepancy at backward

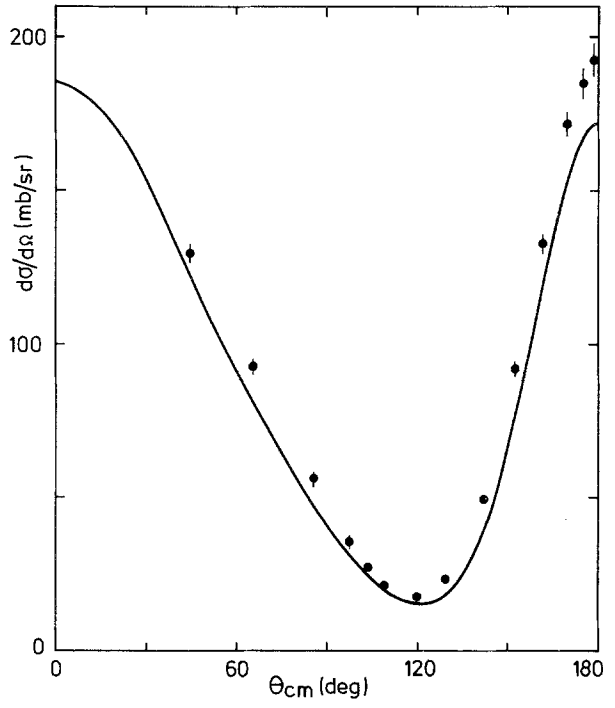

Fig. 3. The differential cross section for *n-d* elastic scattering. The theoretical result for $E_n = 10.3$ MeV (solid line) is based on the large set of forces. Closed circles are experimental data at $E_n = 10.25$ MeV taken from ref. [29]

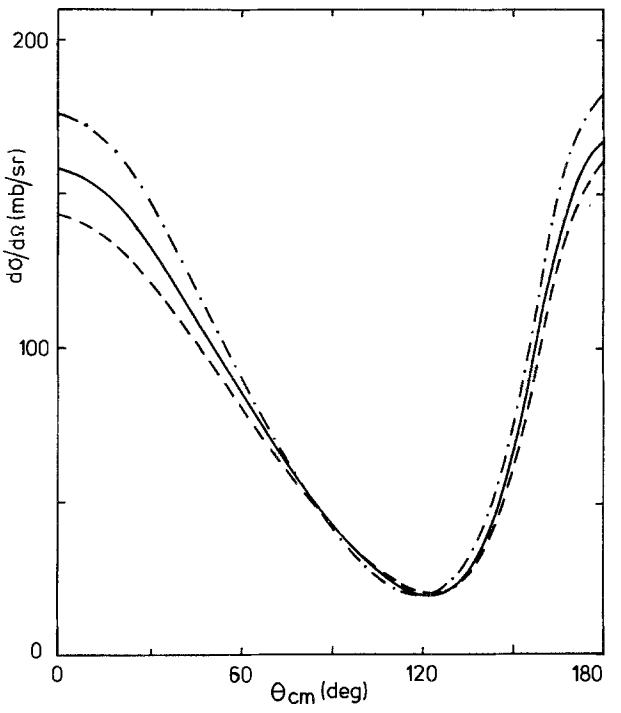

Fig. 4. The differential cross section for *n-d* elastic scattering. Different lines represent theoretical predictions at $E_n = 10$ MeV: solid line for all waves $^1S_0$, $^3S_1$-$^3D_1$, $^3P_0$ and $^3P_1$ included, dashed line without $^3P_0$ wave and dashed-dotted line without $^3P_1$ wave

angles and also around 70°. We demonstrate in Fig. 4 the sensitivity of the differential cross section with respect to different *p*-wave contributions. The calculation is performed at $E_n = 10.0$ MeV and is based on two-nucleon forces corresponding to the small set. In going from the operator T to the operator U (see Eq. (8)) we kept either all partial waves in T (solid line) or dropped just the waves

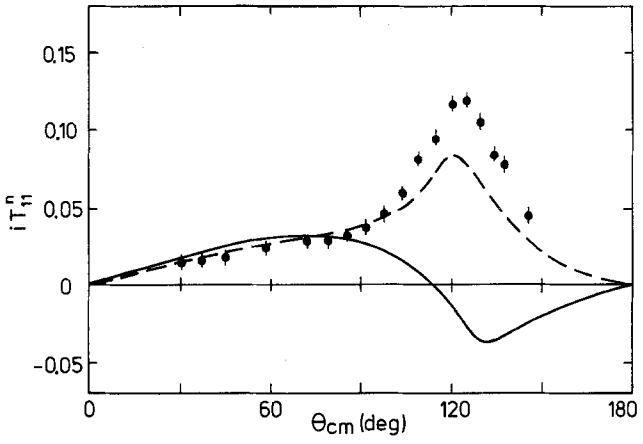

Fig. 5. The angular distribution of the neutron analyzing power iT_{11}^n for *n-d* elastic scattering. Closed circles are experimental data at $E_n = 10.0$ MeV taken from ref. [18]. The dashed curve is based on the large set and calculated at $E_n = 10.3$ MeV. The solid curve is based on the small set and calculated at $E_n = 10.0$ MeV

with $^3P_0$ (dashed line) or with $^3P_1$ (dashed-dotted line). Note that the two cases are not based on different dynamical calculations determining T. It is apparent that the inclusion of the p-states is especially important at forward and backward angles.

In Fig. 5 we show the elastic neutron analyzing power iT_{11}^n ($iT_{11}^n = (\sqrt{2}/2)A_y^n$). The experimental data are from ref. [18] taken at $E_n = 10.0$ MeV. The dashed curve calculated for $E_n = 10.31$ MeV shows nice agreement up to $\theta = 80°$ but is nearly a factor of 1.5 too small in the maximum. As is demonstrated in ref. [18] the maximum region results from a complicated interference of amplitudes derived from p-wave forces. We can reconfirm that sensitivity in showing iT_{11}^n from a calculation based on two-body forces of the small set (solid curve). That calculation was done at $E_n = 10.0$ MeV.

It will be interesting to redo the calculation for the Paris potential, where theoretical results [18] are available gained through finite rank approximations of the force. There the disagreement in the maximum of the analyzing power is much less.

We have studied also the problem of how many total angular momentum states are to be included in the calculation of different observables. As a measure we use

$$X = \frac{A(J \leqslant J_1) - A(J \leqslant J_2)}{A(J \leqslant J_1)} \times 100\% , \tag{15}$$

where $A(J \leqslant J_i)$ denotes the observable A calculated on the basis of including J-states up to J_i. We calculate X for different observables as a function of J_2 at given $J_1 = \frac{15}{2}$. The amplitudes used are generated at $E_n = 10.0$ MeV with the small set of two-body forces. It is found that the differential cross section and the elastic analyzing powers are well described choosing $J_{\max} = \frac{15}{2}$. As an example we show X for iT_{11}^n in Fig. 6.

Experimental data for neutron induced deuteron break-up are poor in comparison to elastic data. Up to now there exist only few sets of cross section measurements for kinematically complete setups [30]. Measurements of neutron analyzing powers in the break-up process are under discussion and therefore theoretical predictions are highly desirable. We show in Fig. 7 as an example the tensor analyzing power T_{20} in the space-star configuration. This is a break-up configuration, where the three nucleons have equal magnitudes of the momenta in

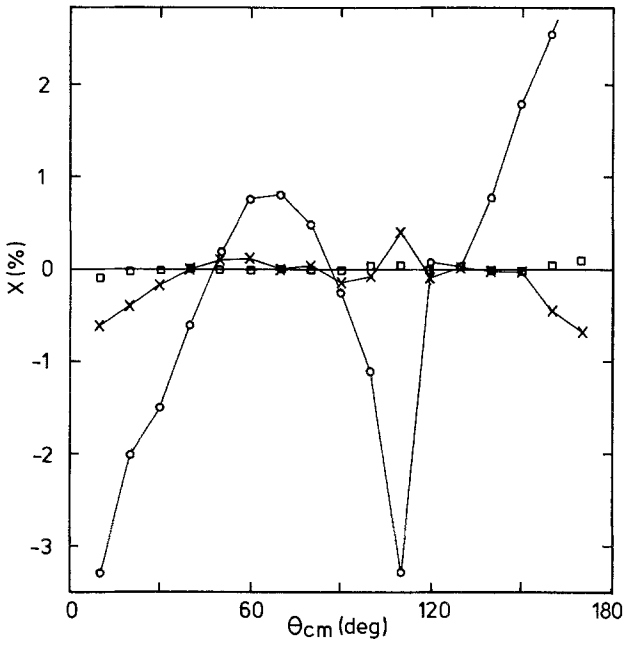

Fig. 6. Convergence of neutron analyzing power iT_{11}^n for *n-d* elastic scattering (solid curve in Fig. 5) with respect to total angular momentum J. The definition of X is given in the text. These percentage deviations were obtained with $J_1 = \frac{15}{2}$ for different J_2 values: circles for $J_2 = \frac{9}{2}$, crosses for $J_2 = \frac{11}{2}$, squares for $J_2 = \frac{13}{2}$

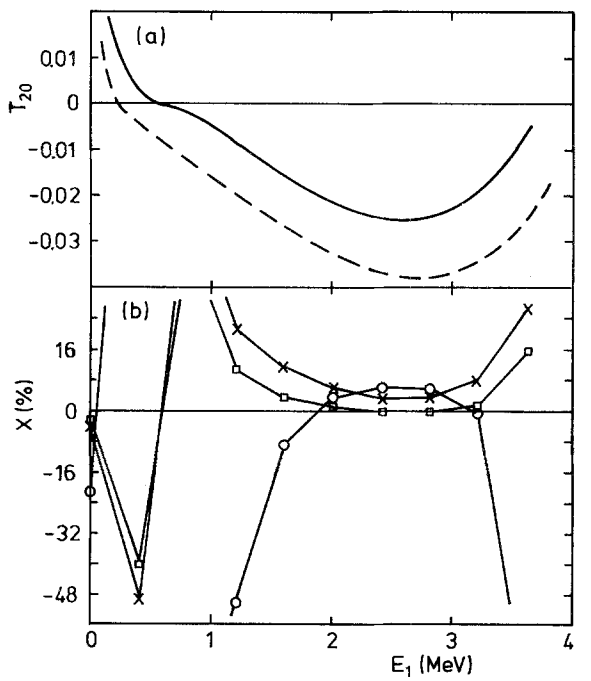

Fig. 7. The neutron-induced deuteron break-up $d(n,nn)p$ in the space-star geometry $\theta_{n_1} = \theta_{n_2} = 48.9°$, $\phi_{n_{12}} = 120°$. In **a** the deuteron analyzing power T_{20} is shown for the large set at $E_n = 10.3$ MeV (dashed curve) and for the small set at $E_n = 10.0$ MeV (solid curve). In **b** the convergence with respect to J of T_{20} obtained with small set is shown. The meaning of different symbols in **b** is the same as in Fig. 6

the c.m. system and lie in the plane perpendicular to the beam direction. The dashed curve refers to $E_n = 10.31$ MeV and includes the large set of two-body forces. The solid curve refers to $E_n = 10.0$ MeV and is based on the small set. In this case the inclusion of higher partial waves changes significantly the values of T_{20} but does not affect the shape. In the lower part of the figure the quantity X related to the solid curve in **a** is shown. It is evident that $J = \frac{15}{2}$ is not sufficient. The dashed curve, our prediction, is based on $J_{\max} = \frac{17}{2}$.

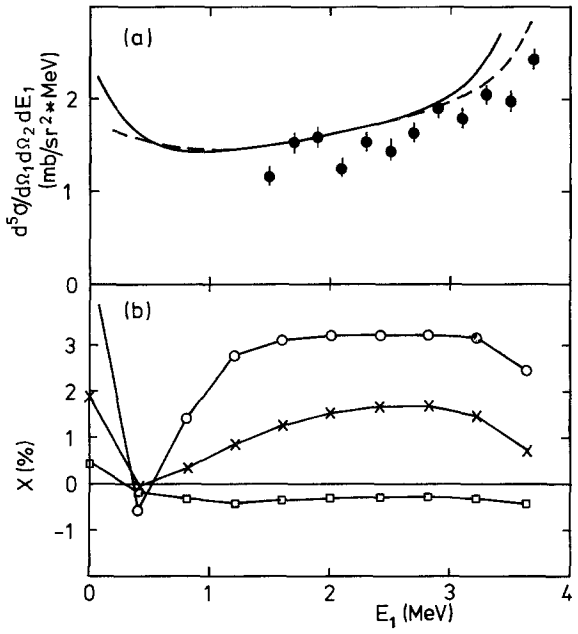

Fig. 8. The neutron-induced deuteron break-up $d(n, nn)p$ in the same geometry as in Fig. 7. In **a** the dashed line is the cross section based on the large set at $E_n = 10.3$ MeV and the dotted line the cross section based on the small set at $E_n = 10.0$ MeV. The closed circles are the experimental data at $E_n = 10.3$ MeV from ref. [31]. In **b** the convergence of the cross section with respect to J is shown. This refers to $E_n = 10.0$ MeV and the small set. The meaning of different symbols in **b** is the same as in Fig. 6

The break-up cross section in the same star configuration is less demanding as seen in the lower part of Fig. 8. There the quantity X is shown for a calculation at $E_n = 10.0$ MeV with the small set of forces. The corresponding break-up cross section is given by the solid line. The dashed curve is based on the large set and calculated at $E_n = 10.31$ MeV. It is compared to the experimental data taken also at $E = 10.3$ MeV [31].

We have presented in this work our first results solving the AGS-equations in momentum space for a meson-theoretical potential in a truncated basis. The inclusion of the two-nucleon forces in all p- and d-waves is important. A more detailed study of the sensitivity to different force components is planned. An investigation for different energies and different N-N potentials is underway and will be published in a forthcoming paper.

Appendix

The matrix elements of the tP operator, which are the zero-order solutions of Eq. (10), are given by

$$\langle pq\alpha|tP|\phi\rangle = \sum_{l_{\alpha'}} \int_{-1}^{1} dx \frac{\langle pl_\alpha|t^{(\alpha)}\left(E - \frac{3}{4m}q^2\right)|\pi_1 l_{\alpha'}\rangle}{\pi_1^{l_{\alpha'}}} \sum_{l_0\lambda_0 I_0} G_{\tilde{\alpha}\alpha_0}(q, q_0, x)\frac{\varphi_{l_0}(\pi_2)}{\pi_2^{l_0}} C_{\alpha_0}^{m_n m_d}, \quad \text{(A.1)}$$

where

$$\alpha_0 = \{(l_0 1)1(\lambda_0 \tfrac{1}{2})I_0(1I_0)J(0\tfrac{1}{2})\tfrac{1}{2}\}$$

and

$$C_{\alpha_0}^{m_n m_d} = \sqrt{\frac{2\lambda_0 + 1}{4\pi}}\langle \lambda_0 0 \tfrac{1}{2} m_n | I_0 m_n\rangle\langle 1 m_d I_0 m_n | J m_n + m_d\rangle . \quad \text{(A.2)}$$

It is assumed that the incoming momentum $\mathbf{q}_0$ is directed along the z-axis. The quantity $\varphi_{l_0}(p)$ is the internal deuteron wave function in the momentum representation.

References

1. Reid, R. V.: Ann. Phys. (NY) **50**, 411 (1968)
2. Lacombe, M., Loiseau, B., Richard, J. M., Vinh Mau, R., Côté, J., Pirès, P., de Tourreil, R.: Phys. Rev. **C21**, 861 (1980)
3. Erkelenz, K.: Phys. Rep. **13**, 191 (1974); Holinde, K., Machleidt, R.: Nucl. Phys. **A247**, 495 (1975)
4. Laverne, A., Gignoux, C.: Nucl. Phys. **A203**, 597 (1973); Brandenburg, R. A., Kim, Y. E., Tubis, A.: Phys. Rev. **C12**, 1368 (1975); Brandenburg, R. A., Sauer, P. U., Machleidt, R.: Z. Phys. **A208**, 93 (1977); Afnan, I. R., Birrell, N. D.: Phys. Rev. **C16**, 823 (1977); Payne, G. L., Friar, J. L., Gibson, B. F., Afnan, I. R.: Phys. Rev. **C22**, 820 (1980); Hajduk, C., Sauer, P. U.: Nucl. Phys. **A369**, 321 (1981); Glöckle, W.: Nucl. Phys. **A381**, 343 (1982); Ishikawa, S., Sasakawa, T., Sawada, T., Ueda, T.: Phys. Rev. Lett. **53**, 1877 (1984); Bömelburg, A.: Phys. Rev. **C34**, 14 (1986)
5. Friar, J. L.: in: Theoretical and Experimental Investigations of Hadronic Few-Body Systems (Ciofi degli Atti, C., Benhar, O., Pace, E., Salmè, G., eds.), (Few-Body Systems, Suppl. 1), p. 94. Wien-New York: Springer 1986; Sasakawa, T.: ibid., p. 105
6. Zabolitzky, J. G.: Nucl. Phys. **A228**, 272 (1974); **A228**, 285 (1974); Kümmel, H., Lührmann, K. H., Zabolitzky, J. G.: Phys. Rep. **C36**, 1 (1978); Tjon, J. A.: Phys. Rev. Lett. **40**, 1239 (1978); Carlson, J., Pandharipande, V. R., Wiringa, R. B.: Nucl. Phys. **A481**, 59 (1983); Wiringa, R. B.: Nucl. Phys. **A401**, 86 (1983); Wiringa, R. B.: in: Theoretical and Experimental Investigations of Hadronic Few-Body Systems (Ciofi degli Atti, C., Benhar, O., Pace, E., Salmè, G., eds.), (Few-Body Systems, Suppl. 1), p. 130. Wien-New York: Springer 1986; Akaishi, Y.: ibid., p. 120; Ballot, J. L.: ibid., p. 140
7. Machleidt, R., Holinde, K., Elster, Ch.: Phys. Rep. **149**, 1 (1987)
8. Sasakawa, T.: Nucl. Phys. **A463**, 327c (1987); Brandenburg, R. A., Chulick, G. S., Machleidt, R., Picklesimer, A., Thaler, R. M.: Los Alamos Preprint LA-Ur-86-3700; Bömelburg, A.: private communication
9. Sasakawa, T., Ishikawa, S.: Few-Body Systems **1**, 3 (1986); Bömelburg, A.: Phys. Rev. **C34**, 14 (1986); Chen, C. R., Payne, G. L., Friar, J. L., Gibson, B. F.: Phys. Rev. **C33**, 1740 (1986); Gibson, B. F.: in: The Three-Body Force in the Three-Nucleon System (Berman, B. L., Gibson, B. F., eds.), (Lecture Notes in Physics, Vol. 260), p. 511. Berlin-Heidelberg-New York-Tokyo: Springer 1986
10. Pandharipande, V. R.: in: The Three-Body Force in the Three-Nucleon System (Berman, B. L., Gibson, B. F., eds.), (Lecture Notes in Physics, Vol. 260), p. 59. Berlin-Heidelberg-New York-Tokyo: Springer 1986
11. Arisaka, I., Katayama, T., Nakagawa, K., Obinata, T.: Prog. Theor. Phys. **77**, 106 (1987)
12. Faddeev, L. D.: Soviet Phys. JETP **12**, 1014 (1961)
13. Amado, R. D.: Phys. Rev. **132**, 485 (1963); Aaron, R. A., Amado, R. D.: Phys. Rev. **150**, 857 (1966)
14. Lovelace, C.: Phys. Rev. **B135**, 1225 (1964)
15. Alt, E. O., Grassberger, P., Sandhas, W.: Nucl. Phys. **B2**, 167 (1967)
16. Plessas, W.: in: Proc. Int. Symp. on Few-Body Methods and Their Application in Atomic, Molecular and Nuclear Physics and Chemistry, Nanning, 1986 (Lim, T.-K., et al., eds.), p. 43. Singapore: World Scientific 1986
17. Plessas, W., Haidenbauer, J., Koike, Y.: in: Theoretical and Experimental Investigations of Hadronic Few-Body Systems (Ciofi degli Atti, C., Benhar, O., Pace, E., Salmè, G., eds.), (Few-Body Systems, Supp. 1), p. 172. Wien-New York: Springer 1986; Koike, Y., Haidenbauer, J., Plessas, W.: Phys. Rev. **C35**, 396 (1987)
18. Howell, C. R., Tornow, W., Murphy, K., Pfitzner, H. G., Roberts, M. L., Anli Li, Felsher, P. D., Walter, R. L., Šlaus, I., Treado, P. A., Koike, Y.: Few-Body Systems **2**, 19 (1987)
19. Kloet, W. M., Tjon, J. A.: Nucl. Phys. **A210**, 380 (1973)
20. Stolk, C., Tjon, J. A.: Nucl. Phys. **A319**, 1 (1979)
21. Benayoun, J. J., Chauvin, J., Gignoux, C., Laverne, A.: Phys. Rev. Lett. **36**, 1438 (1976)
22. Takemiya, T.: Prog. Theor. Phys. **74**, 301 (1985)

23. Brandenburg, R. A.: Few-Body Systems **3**, 59 (1987)
24. Böttcher, J., et al.: Verh. DPG (VI) **21**, 454 (1986); Howell, C. R., Šlaus, I., Tornow, W., Treado, P. A., Lambert, J. M., Nagui, A., Walter, R. L.: in: The Three-Body Force in the Three-Nucleon System (Berman, B. L., Gibson, B. F., eds.), (Lecture Notes in Physics, Vol. 260), p. 229. Berlin-Heidelberg-New York-Tokyo: Springer 1986
25. Glöckle, W.: The Quantum-Mechanical Few-Body Problem. Berlin-Heidelberg-New York-Tokyo: Springer 1983
26. Kloet, W. M., Tjon, J. A.: Ann. Phys. **79**, 407 (1973); Bömelburg, A., Glöckle, W., Meier, W.: in: Few-Body Problems in Physics, Vol. II: Contributed Papers (Zeitnitz, B., ed.), p. 483. Amsterdam: Elsevier 1984
27. Simonius, M.: in: Polarization Nuclear Physics (Fick, D., ed.), (Lecture Notes in Physics, Vol. 30), p. 38. Berlin-Heidelberg-New York: Springer 1974
28. Glöckle, W., Hasberg, G., Neghabian, A. R.: Z. Phys. **A305**, 217 (1982)
29. Schwarz, P., Klages, H. O., Doll, P., Haesner, B., Wilczynski, J., Zeitnitz, B., Kecskemeti, J.: Nucl. Phys. **A398**, 1 (1983)
30. Klages, H. O.: in: The Three-Body Force in the Three-Nucleon System (Berman, B. L., Gibson, B. F., eds.), (Lecture Notes in Physics, Vol. 260), p. 203. Berlin-Heidelberg-New York-Tokyo: Springer 1986
31. Bodek, K., Kamke, D., Krug, J., Lübcke, W., Obermanns, S., Rühl, H., Steinke, M., Stephan, M., Szczurek, A.: in: The Three-Body Force in the Three-Nucleon System (Berman, B. L., Gibson, B. F., eds.), (Lecture Notes in Physics, Vol. 260), p. 307. Berlin-Heidelberg-New York-Tokyo: Springer 1986

Received August 10, 1987; accepted for publication September 8, 1987